



Published in final edited form as:

Adv Funct Mater. 2011 June 7; 21(11): 2118–2128. doi:10.1002/adfm.201002711.

Critical Property in Relaxor-PbTiO₃ Single Crystals --- Shear Piezoelectric Response

Fei Li[Prof.],

Electronic Materials Research Laboratory, Xi'an Jiaotong University, Xi'an 710049 (P. R. China)

Materials Research Institute, Pennsylvania State University, University park PA 16802 (USA)

Shujun Zhang[Prof.],

Materials Research Institute, Pennsylvania State University, University park PA 16802 (USA)

Zhuo Xu[Prof.],

Electronic Materials Research Laboratory, Xi'an Jiaotong University, Xi'an 710049 (P. R. China)

Xiaoyong Wei, and

Electronic Materials Research Laboratory, Xi'an Jiaotong University, Xi'an 710049 (P. R. China)

Thomas R. Shroud

Materials Research Institute, Pennsylvania State University, University park PA 16802 (USA)

Shujun Zhang: soz1@psu.edu

Abstract

The shear piezoelectric behavior in relaxor-PbTiO₃ (PT) single crystals is investigated in regard to crystal phase. High levels of shear piezoelectric activity, d_{15} or $d_{24} > 2000$ pC N⁻¹, has been observed for single domain rhombohedral (R), orthorhombic (O) and tetragonal (T) relaxor-PT crystals. The high piezoelectric response is attributed to a flattening of the Gibbs free energy at compositions proximate to the morphotropic phase boundaries, where the polarization rotation is easy with applying perpendicular electric field. The shear piezoelectric behavior of perovskite ferroelectric crystals was discussed with respect to ferroelectric-ferroelectric phase transitions and dc bias field using phenomenological approach. The relationship between single domain shear piezoelectric response and piezoelectric activities in domain engineered configurations were given in this paper. From an application viewpoint, the temperature and ac field drive stability for shear piezoelectric responses are investigated. A temperature independent shear piezoelectric response (d_{24} , in the range of -50°C to O-T phase transition temperature) is thermodynamically expected and experimentally confirmed in orthorhombic relaxor-PT crystals; relatively high ac field drive stability (5 kV cm⁻¹) is obtained in manganese modified relaxor-PT crystals. For all thickness shear vibration modes, the mechanical quality factor Q_s are less than 50, corresponding to the facilitated polarization rotation.

Keywords

Dielectrics; Ferroics; Relaxor-PT; Shear piezoelectric response

1. Introduction

Relaxor-PbTiO₃ (PT) based ferroelectric single crystals, such as (1-x)Pb(Zn_{1/3}Nb_{2/3})O₃-xPbTiO₃ (PZN-PT) and (1-x)Pb(Mg_{1/3}Nb_{2/3})O₃-xPbTiO₃ (PMN-PT) have attracted considerable interest over the last decade due to their superior piezoelectric properties compared to commercial piezoelectric ceramics, including (1-x)PbZrO₃-xPbTiO₃ (PZT). The ultrahigh piezoelectric response ($d_{33} > 1500$ pC N⁻¹, $k_{33} > 95\%$) was found to be along the [001] crystallographic direction for compositions lying in proximity to a morphotropic phase boundary (MPB).^[1-7] In contrast to polycrystalline piezoelectric ceramics, high piezoelectric activities in relaxor-PT based crystals is believed to be intrinsic in nature.^[7] Two intrinsic based mechanisms have been proposed to explain the origin of the high piezoelectric response. The first one is ‘polarization rotation’,^[8-10] where the high piezoelectric response is attributed to an ‘ease’ in polarization rotation process. It is believed that the monoclinic (M) phase^[10-16] acts as a bridge between the morphotropic phases [rhombohedral (R) and tetragonal (T)], facilitating the polarization rotation.^[10-12, 17, 18] For the second intrinsic mechanism, the high piezoelectric response has been attributed to the high level of shear piezoelectric response in the single domain state,^[19] which can greatly contribute to the longitudinal piezoelectric response in [001] and [011] domain engineered crystals. As analyzed by Damjanovic et al,^[20-23] the high shear piezoelectric activity is due to a flattening of the free energy profile (instability of free energy) near the MPB.

From an application viewpoint, the investigation of relaxor-PT crystals has been focused on crystal growth technology and usage temperature range. Relaxor-PT based crystals with large size, homogeneous composition, and low cost are desirable for various applications. To date, the PMN-PT and Pb(In_{1/2}Nb_{1/2})O₃-Pb(Mg_{1/3}Nb_{2/3})O₃-PbTiO₃ (PIN-PMN-PT) crystals can be grown with relatively large size (3-inch in diameter) using the modified Bridgman method.^[24-25] It was also reported that a continuous feeding technique can be used to grow relaxor-PT based crystals with uniform composition and properties.^[26] For commercial PMN-PT crystals, the temperature usage range is limited by the ferroelectric-ferroelectric phase transition temperature T_{R-T} , $< 95^{\circ}\text{C}$.^[6] In recent years, ternary PIN-PMN-PT crystals were grown and investigated, showing a broadened temperature usage range ($T_{R-T} \sim 120^{\circ}\text{C}$).^[27-32] To further enhance the usage temperature range for relaxor-PT crystals, efforts have been put into the tetragonal PIN-PMN-PT crystals, in which, broadened temperature usage range ($> 200^{\circ}\text{C}$), together with good electromechanical coupling k_{33} ($\sim 84\%$), were observed, since no ferroelectric-ferroelectric phase transition occurs above room temperature.^[33]

Until now, piezoelectric investigations for relaxor-PT based crystals have been mainly focused on their longitudinal behaviors, while the transverse (shear) piezoelectric and dielectric properties of relaxor-PT crystals were limited,^[34-38] which have not been extensively studied yet. In contrast to longitudinal mode, the level of transverse (shear) piezoelectric/dielectric response is much higher,^[34-39] making relaxor-PT based crystals good candidates for various shear mode applications, such as vector sensors, non-destructive evaluation (NDE) transducers and low frequency sonar. Furthermore, the shear piezoelectric activity of single domain state is believed to be a critical factor for the origin of the high longitudinal piezoelectric response in domain engineered state. Thus, it is desirable to systematically study the shear properties in relaxor-PT crystals.

In this paper, recent progresses on studying the piezoelectric shear response of relaxor-PT based crystals were surveyed. The shear piezoelectric behavior is analyzed with respect to the polarization rotation process, including the temperature and composition dependence of shear properties, the contribution of shear piezoelectric to longitudinal piezoelectric in domain engineered crystals, and shear piezoelectricity in domain engineered states. From an

application viewpoint, the temperature and ac field drive stability, mechanical quality factor Q of the shear vibration modes were measured and discussed. Approaches to improve the temperature and ac field drive stability were also proposed.

2. Shear piezoelectric behavior in relaxor-PT based ferroelectric crystals

2.1. Shear piezoelectric behaviors in single domain configuration

The shear piezoelectric properties in relaxor-PT based crystals were studied for various ferroelectric phases, including the rhombohedral (R), orthorhombic (O), and tetragonal (T) phases. Fig. 1 shows the schematic phase diagram, showing R, O, T ferroelectric phases and paraelectric phase (P) (The monoclinic M_C phase was found to be only a slightly distorted from orthorhombic phase. Thus, after poled along [011] direction, it was proper to consider the M_C phase as a quasi-orthorhombic phase for analysis).^[14, 15] The spontaneous polarization vectors of rhombohedral, orthorhombic and tetragonal crystals lie along $[111]_C$, $[011]_C$ and $[001]_C$ crystallographic directions respectively, as depicted in Fig. 1. For the rhombohedral, orthorhombic and tetragonal crystals by poling along their respective polar directions, the symmetry is 3m with one independent shear piezoelectric coefficient ($d_{15}=d_{24}$), mm2 with two independent shear coefficients ($d_{15}\neq d_{24}$) and 4mm with one independent shear coefficient ($d_{15}=d_{24}$), respectively. Table 1 summarized the shear piezoelectric coefficients of rhombohedral, orthorhombic and tetragonal phases for PIN-PMN-PT crystals with the compositions around MPB.^[33, 40] High shear piezoelectric coefficients (>2000 pC N⁻¹) and electromechanical coupling factors ($>85\%$) were observed at room temperature for all single domain crystals, including rhombohedral '1R', orthorhombic '1O' and tetragonal '1T' domain configuration.

In ferroelectric crystals, with applying electric field perpendicular to polar direction, the polarization will rotate in order to minimize the free energy,^[41] leading to a shear deformation of the lattice, as depicted in Fig. 2. For single domain relaxor-PT crystals, therefore, the shear piezoelectric response is associated with the polarization rotation processes.^[22] As analyzed in the following, the polarization rotation process becomes easy with the composition close to the MPB, leading to a high level of shear piezoelectric activity.

2.2. Role of ferroelectric-ferroelectric phase transitions for shear piezoelectric response

From a thermodynamic analysis on perovskite ferroelectric crystals, the shear piezoelectric coefficients generally exhibit maximum values around the ferroelectric-ferroelectric phase transitions, no matter it is induced by the composition or temperature, due to the flattening of free energy profile or the enhanced energy instability around the phase transition points,^[20-23] as depicted in Fig. 3. Based on previous measurements and thermodynamic analysis,^[20, 40, 42] the characteristics of shear piezoelectric coefficients in rhombohedral, orthorhombic, and tetragonal crystals are summarized in the following:

1. In the rhombohedral phase, only one independent piezoelectric coefficient d_{15} for 3m symmetry, increasing as the composition/temperature approaches the orthorhombic or tetragonal phase from the rhombohedral side, (for example, d_{15} increase with increasing temperature);
2. For the tetragonal phase with 4mm symmetry, the independent shear piezoelectric coefficient d_{15} will increase as the composition/temperature approaches the rhombohedral or orthorhombic phase, (for example, d_{15} increase with decreasing temperature);
3. In orthorhombic crystals with mm2 symmetry, there are two independent shear piezoelectric coefficients, d_{15} and d_{24} . As shown in Fig. 4,^[40] due to the different

polarization rotation paths, the coefficient d_{15} will increase with the composition/temperature close to the O-T phase boundary, while d_{24} will be enhanced with the composition/temperature close to the O-R phase boundary/phase transition temperature.

The above discussion can be used as a basis to analyze the temperature/composition dependent shear properties for relaxor-PT based crystals with different phases.

2.3. Shear piezoelectric behaviors in domain engineered crystals

In contrast to the high level of shear piezoelectric responses in single domain crystals, both high and low shear coefficients were observed in domain engineered crystals. (for example, in $[001]_C$ poled rhombohedral crystals, $d_{15}^* < 200 \text{ pC N}^{-1}$; [43–44] in $[011]_C$ poled rhombohedral crystals, $d_{15}^* > 2000 \text{ pC N}^{-1}$ while $d_{24}^* < 200 \text{ pC N}^{-1}$ [45–46]). The properties of the multi-domain crystals can be attributed to the single domain properties and related domain configurations, i. e., orientation and structure of the domains. In order to evaluate the difference in single and multi-domain configurations, the shear properties of $[011]_C$ poled rhombohedral crystals were analyzed. [47] Fig. 5 shows the domain configuration for $[011]_C$ poled rhombohedral crystals, where the domain configuration is noted as ‘2R’, with mm2 macro-symmetry. The remained 71° domains in ‘2R’ domain configuration are designated as domain I and domain II. For 15-mode, domains I and II are equivalent to the perpendicular electric field E_1 , as shown in Fig. 6. The polarization rotation of both domains I and II contribute to the shear piezoelectric deformation S_5 , leading to a high shear coefficient d_{15}^* . However, for the 24-mode, the contribution to the shear deformation S_4 via polarization rotation of domains I and II are opposed, negating one another, as depicted in Fig. 6. [47] Thus, the coefficient d_{24}^* is relatively small in $[011]_C$ poled domain engineered crystals. [45–47] Analogous to the above analysis, the small shear piezoelectric coefficient d_{15}^* in $[001]_C$ poled rhombohedral crystals (with ‘4R’ domain configuration) can be expected.

In summary, the high shear piezoelectric behaviors for single domain rhombohedral, orthorhombic and tetragonal crystals with compositions around MPBs, are a result of flattening of the free energy profile. The low level of shear piezoelectric responses in domain engineered crystals can be explained by the negating effect among different domain rotation processes.

2.4. Shear vs. longitudinal piezoelectric response

The high longitudinal piezoelectric response is generally observed along the non-polar direction(s) in relaxor-PT based crystals. [1, 48] Taking $[011]_C$ poled tetragonal crystals as example, the enhanced piezoelectric response in these domain engineered crystals are illustrated in Fig. 7. The electric field along non-polar $[011]_C$ direction can be separated into two parts: E_{\parallel} , E_{\perp} . The E_{\parallel} is along the polar direction and leads the polarization extension; E_{\perp} gives rise to the polarization rotation and consequently the shear deformation of single domain. This shear deformation can contribute to the longitudinal strain along $[011]_C$ direction. Thus, if the related shear piezoelectric response of single domain is high, the longitudinal piezoelectric response along the non-polar direction would be greatly enhanced. Based on the single domain properties, [33, 45, 49] Fig. 8 shows the orientation dependence of the longitudinal piezoelectric coefficient d_{33}^* for PIN-PMN-PT crystals. It can be seen that the maximum d_{33}^* values are along non-polar directions for all three different phases. As demonstrated, [22–23] if the piezoelectric anisotropy factor, d_{15}/d_{33} , is greater than 2, the maximum longitudinal piezoelectric coefficient will be along non-polar direction, and this type of crystals is referred to ‘rotator’ ferroelectrics. The anisotropic factors and electromechanical properties of various single domain and domain engineered configurations are listed in Table 2 (data from Ref. [39], [33–34], [47–51]). For the

rhombohedral and orthorhombic crystals, both longitudinal piezoelectric coefficients and coupling factors are enhanced in domain engineered configurations, due to the high piezoelectric anisotropy. It is worth noting that although the piezoelectric coefficients are enhanced for domain engineered tetragonal crystals, the maximum coupling factors k_{33}^* were yet along the $[001]_C$ polar direction, this is due to the dielectric anisotropy being greater than the piezoelectric anisotropy factor.^[22, 48, 52]

According to the above analysis, the shear piezoelectric response contributes to the longitudinal piezoelectric response in domain engineered crystals. Furthermore, by Rayleigh analysis of domain engineered relaxor-PT crystals, the ultrahigh longitudinal piezoelectric response for domain engineered crystals is mainly attributed to the single domain shear piezoelectric response.^[7, 53–54] In addition, the shear piezoelectric responses generally exhibit maximum values around MPBs based on the thermodynamic analysis, thus the longitudinal piezoelectric response in domain engineered crystals will be greatly enhanced as the composition approaches MPBs.

3. Temperature dependent dielectric and piezoelectric properties

Based on the discussion in section 2.2 and phase diagram of the relaxor-PT based crystals (Fig. 1), the temperature dependent shear dielectric and piezoelectric properties were investigated for rhombohedral, orthorhombic, and tetragonal crystals, respectively.

For rhombohedral crystals, as presented in section 2.2, the shear piezoelectric coefficient d_{15} increases with temperature increasing, due to the phase approaches R-T MPB region with increasing temperature. For tetragonal crystals, however, due to the T-O ferroelectric phase transition lying below room temperature, the shear piezoelectric coefficient d_{15} is expected to decrease with increasing temperature, moving away from T-O MPB region. For $[011]_C$ poled orthorhombic crystals, the coefficient d_{15} should increase with temperature increasing, due to the O-T phase transition occurs above room temperature. Of particular interest is that a temperature independent d_{24} can be expected in orthorhombic crystals, due to a compositionally ‘vertical’ O-R phase boundary exists for relaxor-PT based crystals, as shown in Fig. 1, revealing that no O-R phase transition occurs in the studied temperature range for orthorhombic relaxor-PT crystals.^[40]

Fig. 9 shows the shear piezoelectric behavior for rhombohedral, orthorhombic, and tetragonal PIN-PMN-PT crystals as a function of temperature. The variations of the shear piezoelectric coefficients for PIN-PMN-PT based crystals are consistent with the above analysis. The temperature independent shear piezoelectric coefficient (d_{24}), together with its ultrahigh value $>2000 \text{ pC N}^{-1}$, was observed.^[40] The piezoelectric coefficients d_{15} for rhombohedral and orthorhombic crystals were found to increase with increasing temperature, due to which, the longitudinal piezoelectric coefficients d_{33}^* along $[001]_C$ direction were expected to increase with increasing temperature (below the $T_{R-T/O-T}$).^[6, 29, 54–58] On the other hand, for domain engineered tetragonal crystals (poled along $[011]_C$ direction), the coefficient d_{33}^* was found to decrease as temperature increases, due to the decreased d_{15} , as shown in Fig. 9b.^[48] It is worth noting that temperature independent longitudinal coefficient d_{33}^* can be expected in the crystals with single domain state (poled along polar direction), where no shear piezoelectric contribution was observed, for example, in $[001]_C$ poled tetragonal PIN-PMN-PT crystals, the d_{33}^* maintain the same values up to 200°C .^[33]

The temperature dependent dielectric permittivity and coupling factors are shown in Fig. 10. The temperature characteristics of dielectric permittivities exhibited similar trend to piezoelectric coefficients, as predicted by thermodynamic analysis. The dielectric permittivity ϵ_{22}/ϵ_0 of orthorhombic crystals was found to be temperature independent, while

permittivity $\varepsilon_{11}/\varepsilon_0$ of rhombohedral, orthorhombic and tetragonal crystals showing large variations with temperature.

Due to the similar variation tendency of dielectric and piezoelectric response, the electromechanical coupling factors ($k \propto d/\varepsilon^{1/2}$) were relatively stable with respect to temperature, as shown in Fig. 10(b), where the shear coupling factor k_{15} of tetragonal PIN-PMN-PT crystal was found to decrease 7% upon temperature from -50°C to 120°C , while the variation of other shear coupling factors was less than 3%.

4. Electric field dependent piezoelectric properties

It is desirable to understand the piezoelectric behaviors in relaxor-PT single crystals under high electric field, including dc bias field and ac drive field, for the potential high power applications, where the field stability needs to be demonstrated.

4.1 Shear piezoelectric response with respect to dc bias field

Under dc bias field, the free energy of perovskite systems can be expressed as follows:^[42]

$$\begin{aligned} \Delta G = & \alpha_1(p_1^2 \\ & + p_2^2 + p_3^2) + \alpha_{11}(p_1^4 \\ & + p_2^4 + p_3^4) + \alpha_{12}(p_1^2 p_2^2 + p_2^2 p_3^2 + p_3^2 p_1^2) \\ & + \alpha_{111}(p_1^6 \\ & + p_2^6 + p_3^6) + \alpha_{112}(p_1^4 p_2^2 \\ & + p_1^2 p_2^4 \\ & + p_2^4 p_3^2 \\ & + p_2^2 p_3^4 \\ & + p_3^4 p_1^2 \\ & + p_3^2 p_1^4) \\ & + \alpha_{123} p_1^2 p_2^2 p_3^2 \\ & - E_1 P_1 - E_2 P_2 - E_3 P_3 \end{aligned} \quad (1)$$

where p_i are the orthogonal components of polarization, measured parallel to the pseudocubic axes of the perovskite unit cell, E_i represents the applied electric field. According to Eq. (1), the energy profiles of PZT40/60 with rhombohedral phase were plotted under the electric field parallel and perpendicular to the [111] polar direction, as shown in Fig. 11. For zero electric field, the minimum free energy exists at the polar vector along $\langle 111 \rangle$ directions ($|p_1|=|p_2|$), indicating that rhombohedral phase is the equilibrium state. Meanwhile, the tetragonal state with polar vector along [001] direction ($p_1=0$) and the polarization rotation path from R to T phase are also marked in Fig. 11.

With applying the electric field along $\langle 111 \rangle$ polar direction, it is observed that the rhombohedral phase becomes more stable due to the lower free energy, which makes the polarization rotation becomes harder, as shown in Fig. 11(b). Based on this notion, the observed reduction of shear piezoelectric coefficient with increasing electric field along [111] direction in rhombohedral PZN-PT crystals can be explained.^[36] On the other hand, in the case of electric field applying perpendicular to polar direction (along [-1-12]), as shown in Fig. 11(c), the free energy of rhombohedral phase (polar vector along [111] direction) increases and the polarization rotation path from R to T phase becomes flatter, indicating the increase in shear piezoelectric response. Thus, an enhanced shear piezoelectric coefficient can be expected with applying perpendicular dc electric field.

4.2 ac electric field stability for shear piezoelectric response

For a high ac field application, the ac field stability of relaxor-PT based crystals is analyzed in the following. Fig. 12 shows the Polarization-Electric field (PE) loops for rhombohedral PIN-PMN-PT crystals as a function of electric field. The small signal impedance characteristics for a thickness shear vibration mode, as a function of ac drive field after 5000th cycling, are shown in Fig. 13. At an electric field below 2 kV cm^{-1} , being half of the coercive field ($E_C \sim 5 \text{ kV cm}^{-1}$), the PE loop after 5000 cycles was found to maintain the same, exhibiting no domain reversal or fatigue in the crystals. The field stability (2 kV cm^{-1}) was also confirmed by the impedance-frequency characteristics, where no change was observed in impedance. With further increasing the level of ac field, the PE loops became nonlinear and exhibited hysteretic behavior, while the anti-resonance frequency was found to shift to lower frequency range, demonstrating the instability of the domain configuration at ac electric field higher than 2 kV cm^{-1} , limiting the crystal usage range $<1/2 E_C$.

To improve the field stability of relaxor-PT based crystals, two approaches have been proposed. The first approach is to use the tetragonal relaxor-PT crystals with improved coercive field ($\sim 9\text{--}11 \text{ kV cm}^{-1}$); the other one is to use ‘acceptor’ modified crystals, where the internal bias field stabilize the polarization.^[59] Both pure and Mn modified PIN-PMN-PT crystals, with rhombohedral, orthorhombic and tetragonal phases, were investigated.^[60] The general properties and ac electric field stability of the PIN-PMN-PT crystals are listed in Table 3. As expected, the ac field stability can be enhanced by both approaches. Of particular interest is that the Mn-modified orthorhombic crystals, where both high electric field drive stability (5 kV cm^{-1}) and piezoelectric coefficient (3500 pC N^{-1}) were obtained.

5. Mechanical quality factor Q for shear vibration modes

The mechanical quality factor Q is an important parameter for high power applications. Thus, the shear mode quality factors for various single domain PIN-PMN-PT crystals were investigated, the results are listed in Table 3. As presented, all quality factors were found to be on the order of 20–30. For comparison, the low quality factors were also observed for the longitudinal mode in domain engineered crystals, being on the order of 100–300.^[48, 61] However, high longitudinal quality factors, being on the order of >2000 , were found in the $[111]_C$ poled single domain rhombohedral^[61] and $[001]_C$ poled single domain tetragonal crystals.^[62] Based on the results, it is proposed that the high level of mechanical losses (low mechanical quality Q) are associated with the polarization rotation process, including the shear mode of single domain crystals and longitudinal mode of domain engineered crystals. The high quality factors observed in longitudinal mode single domain crystals, are due to the lack of polarization rotation process.

In contrast to the piezoelectric coefficient, quality factor Q is more sensitive to some factors, such as the test frequency, electric field level and preload stress.^[63] Of particular interest is that both high level of mechanical quality factor and piezoelectric coefficient were reported in face shear vibration mode (36-mode) of the $[011]_C$ poled rhombohedral crystals,^[64] where the high piezoelectric activity is associated with the polarization rotation process, as shown in Fig. 14. For 36-mode crystals, the applied working electric field is parallel to the poling direction, whereas the working electric field is perpendicular to the poling direction for thickness shear crystals (15-mode, 24-mode). Thus, the mechanical quality factor is also thought to be possibly related to the polarization rotation angle, which is under investigations.

6. Conclusion

The piezoelectric behaviors in relaxor-PT based crystals, with rhombohedral, orthorhombic and tetragonal phases, were investigated. High shear piezoelectric coefficients were generally obtained in single domain rhombohedral, orthorhombic, and tetragonal crystals, with the compositions near MPBs. The high shear piezoelectric activity was a critical characteristic for relaxor-PT based crystals, by which the longitudinal piezoelectric responses were greatly improved in domain engineered crystals.

From application viewpoint, interesting properties were observed for orthorhombic and tetragonal crystals, when compared to their rhombohedral counterpart. The high shear piezoelectric response with improved thermal stability (d_{24}) and ac drive field stability (d_{15} , Mn-modified crystals) were obtained in orthorhombic crystals; meanwhile, the high electromechanical couplings k_{33} (>84%) and mechanical quality factors Q (>2000) were concurrently obtained in tetragonal relaxor-PT crystals, with broadened temperature usage range close to their respective T_C .

7. Experimental

7.1 Poling process

As demonstrated in section II, relaxor-PT crystals were poled along non-polar directions, in order to obtain domain engineered structures for high longitudinal piezoelectric response, while the crystals were poled along polar directions in order to achieve high shear piezoelectric response in single domain structures.

In contrast to domain engineered crystals, such as [001] poled rhombohedral crystals (4R) and [111] poled tetragonal crystals (3T), single domain crystals were found to crack easily during the poling process, limiting their applications.

To design a crack-free poling method for single domain crystals, the domain evolution of tetragonal crystals were analyzed, by poling along [001] polar direction and [111] non-polar directions, respectively.

For tetragonal ferroelectric crystals, six different domains, being along [001], [010], [100], $[-100]$, $[0-10]$, and $[00-1]$ directions, coexist prior to the poling process. As the crystals were poled along [111] direction, domains along $[-100]$, $[0-10]$, and $[00-1]$ directions transformed to the other three electrically favored domains, forming engineered domain configuration '3T', as shown in Fig. 15(a). During the poling process, the electric-field-induced strain by domain switching was minimal, due to the spontaneous strain of these six domains were equivalent with respect to [111] direction.

On the other hand, if the crystals were poled along [001] direction, domains along [010], [100], $[-100]$, $[0-10]$, and $[00-1]$ directions transformed to the electrically favored [001] domain, leading to single domain state '1T', as shown in Fig. 15(b). During this poling process, the electric-field-induced strain was significantly large and abrupt, due to the 90° domain switching from [010], [100], $[-100]$ or $[0-10]$ domains to [001] domain. As expected, the strain was found to be > 0.6%, with a sharp strain- electric field behavior around coercive field, for [001] oriented tetragonal PIN-PMN-PT crystals [33].

According to the above analysis, the crack phenomenon of single domain crystals was attributed to the large strain variation, which was induced by non- 180° (90°) ferroelectric/ferroelastic domain switch. Therefore, in order to avoid cracking, it is necessary to minimize the strain variation during the poling process. Based on this notion, special poling approach

was used to obtain single domain crystals with various ferroelectric phases, as described in the following.

The tetragonal relaxor-PT crystals were poled along [001] direction at the temperature above Curie temperature, and then slowly cooled down to room temperature with the same electric field. By this poling method, only one domain along [001] direction was presented with decreasing temperature from paraelectric to ferroelectric phase. Compared to room temperature poling process, 90° domain switch was avoided in the above poling process.

For rhombohedral and orthorhombic crystals, the poling electric field was applied along [111] and [011] directions, respectively. The crystals were also poled above Curie temperature, where the poling electric field was larger than the tetragonal-rhombohedral/orthorhombic phase transition electric field, in order to guarantee a single domain state with polar vector along [111]/[011] direction for rhombohedral/orthorhombic crystals in the temperature range of $T_C \sim T_{RT}/T_{OT}$.

7.2 Electrical measurements

After the polarization process, the electrodes were removed and re-electrode on the large surfaces, as shown in Table 1. The dielectric permittivity was determined at 1 kHz, using an HP4284A multifrequency LCR meter. The resonance and antiresonance frequencies were measured using an HP4294A impedance-phase gain analyzer. The shear piezoelectric coefficients and electromechanical couplings were determined by resonance and antiresonance frequencies, following IEEE standard. The mechanical quality factor Q was calculated based on the Butterworth-Van Dyke equivalent circuit. High field polarization behaviors were determined using a modified Sawyer-Tower circuit, with measuring frequency of 10Hz, which is much higher than the domain reversal frequency.

Acknowledgments

The authors from Xi'an Jiaotong University acknowledged the National basic research program of China under Grant No. 2009CB623306, the National Natural Science foundation of China under Grant No. 50632030 and 10976022. The work supported by NIH under Grant No. P41-EB21820 and ONR under Grant No. N00014-09-1-01456 and N-00014-07-C-0858.

References

1. Park S-E, Shrout TR. *J. Appl. Phys.* 1997; 82:1804.
2. Park SE, Shrout TR. *Mater. Res. Innovations.* 1997; 1:20.
3. Zhang SJ, Shrout TR. *IEEE Trans. Ultrason. Ferro. Freq. Contr.* 2010; 57:2138.
4. Luo HS, Xu GS, Xu HQ, Wang PC, Yin ZW. *Jpn. J. Appl. Phys.* 2000; 39:5581.
5. Kuwata J, Uchino K, Nomura S. *Jpn. J. Appl. Phys.* 1982; 21:1298.
6. Zhang SJ, Randall CA, Shrout TR. *IEEE Trans. Ultrason. Ferro. Freq. Contr.* 2005; 52:564.
7. Li, Fei; Zhang, S.; Xu, Z.; Wei, X.; Luo, J.; Shrout, TR. *J. Appl. Phys.* 2010; 108 034106.
8. Fu H, Cohen RE. *Nature.* 2000; 403:281. [PubMed: 10659840]
9. Bellaiche L, Garcia A, Vanderbilt D. *Phys. Rev. B.* 2001; 64 060103.
10. Noheda B. *Curr. Opin. Solid State Mater. Sci.* 2002; 6:27.
11. Noheda B, Cox DE, Shirane G, Gonzalo JA, Cross LE, Park S-E. *Appl. Phys. Lett.* 1999; 74:2059.
12. Guo R, Cross LE, Park S-E, Noheda B, Cox DE, Shirane G. *Phys. Rev. Lett.* 2000; 84:5423. [PubMed: 10990959]
13. Xu GS, Luo HS, Xu HQ, Yin ZW. *Phys. Rev. B.* 2001; 64 020102(R).
14. Noheda B, Cox DE, Shirane G, Gao J, Ye Z-G. *Phys. Rev. B.* 2002; 66 054104.
15. La-Orauttapong D, Noheda B, Ye Z-G, Gehring PM, Toulouse J, Cox DE, Shirane G. *Phys. Rev. B.* 2002; 65 144101.

16. Vanderbilt D, Cohen MH. Phys. Rev. B. 2001; 63 094108.
17. Noheda B, Cox DE, Shirane G, Park S-E, Cross LE, Zhong Z. Phys. Rev. Lett. 2001; 86:3891. [PubMed: 11329350]
18. Bellaiche L, Garcia A, Vanderbilt D. Phys. Rev. B. 2001; 64 060103.
19. Damjanovic D, Budimir M, Davis M, Setter N. Appl. Phys. Lett. 2003; 83:527.
20. Budimir M, Damjanovic D, Setter N. J. Appl. Phys. 2003; 94:6753.
21. Budimir M, Damjanovic D, Setter N. Phys. Rev. B. 2005; 72 064107.
22. Davis M, Budimir M, Damjanovic D, Setter N. J. Appl. Phys. 2007; 101 054112.
23. Damjanovic D. IEEE Trans. Ultra. Ferroelectr. Freq. Contr. 2009; 56:1574.
24. Han, P.; Tian, J. Progress in growth of 3-inch diameter PMN-PT crystals. US Navy Workshop on Acoustic Transduction Materials and Devices; The Penn State Conference Center; May, 2006; State College, PA.
25. Luo, J.; Zhang, SJ.; Hackenberger, W.; Shrout, TR. Bridgman Growth and Characterization of Relaxor-PT Piezoelectric Crystals. US Navy Workshop on Acoustic Transduction Materials and Devices; The Penn State Conference Center; May, 2010; State College, PA.
26. Echizenya, K.; Matsushita, M.; Tachi, Y.; Addona, T. Characterization of PMN-PT Single Crystals Grown by Continuous Feed Technique. US Navy Workshop on Acoustic Transduction Materials and Devices; The Penn State Conference Center; May, 2010; State College, PA.
27. Hosono Y, Yamashita Y, Sakamoto H, Ichinose N. Jpn. J. Appl. Phys. 2003; 42(Part 1):5681.
28. Tian J, Han PD, Huang XL, Pan HX. Appl. Phys. Lett. 2007; 91 222903.
29. Zhang SJ, Luo J, Hackenberger W, Shrout TR. J. Appl. Phys. 2008; 104 064106.
30. Zhang SJ, Juo J, Hackengerger W, Sherlock N, Meyer RJ Jr, Shrout TR. J. Appl. Phys. 2009; 105 104506.
31. Xu G, Chen K, Yang D, Li J. Appl. Phys. Lett. 2007; 90 032901.
32. Liu LH, Wu X, Zhao XY, Feng XQ, Jing WP, Luo HS. IEEE Trans. Ultrason. Ferro. Freq. Contr. 2010; 57:2154.
33. Li F, Zhang SJ, Xu Z, Wei X, Luo J, Shrout TR. J. Appl. Phys. 2010; 107 054107.
34. Zhang SJ, Lebrun L, Liu SF, Rhee S, Randall CA, Shrout TR. Jpn. J. Appl. Phys. 2002; 41:L1099.
35. Zhang SJ, Lebrun L, Rhee S, Randall CA, Shrout TR. Appl. Phys. Lett. 2002; 81:892.
36. Liu SF, Ren W, Mukherjee BK, Zhang SJ, Shrout TR, Rehrig PW, Hackenberger WS. Appl. Phys. Lett. 2003; 83:2886.
37. Jin J, Rajan KK, Lim L. IEEE Trans. Ultrason. Ferroelectr. Freq. Contr. 2007; 54:2222.
38. Han PD, Yan WL, Tian J, Huang XL, Pan HX. Appl. Phys. Lett. 2005; 86 052902.
39. Zhang R, Jiang B, Cao W. Appl. Phys. Lett. 2003; 82:3737.
40. Li, Fei; Zhang, S.; Xu, Z.; Wei, X.; Luo, J.; Shrout, TR. Appl. Phys. Lett. 2010; 97 252903.
41. Lines, ME.; Glass, AM. Principles and applications of ferroelectrics and related materials. Clarendon, Oxford: 1979.
42. Haun MJ, Furman ES, Jang J, Cross LE. Ferroelectrics. 1989; 99:13.
43. Liu XZ, Zhang SJ, Luo J, Shrout TR, Cao WW. J. Appl. Phys. 2009; 106 074112.
44. Zhang R, Jiang B, Cao W. J. Appl. Phys. 2001; 90:3471.
45. Zhang R, Jiang B, Jiang W, Cao W. Appl. Phys. Lett. 2006; 89 242908.
46. Sun E, Zhang S, Luo J, Shrout TR, Cao W. Appl. Phys. Lett. 2010; 97 032902.
47. Zhang SJ, Li F, Luo J, Xia R, Hackenberger W, Shrout TR. Appl. Phys. Lett. 2010; 97 132903.
48. Li, Fei; Zhang, S.; Xu, Z.; Wei, X.; Luo, J.; Shrout, TR. J. Am. Ceram. Soc. 2010; 93:2731.
49. Liu X, Zhang SJ, Luo J, Shrout TR, Cao W. Appl. Phys. Lett. 2010; 96 012907.
50. Cao H, Schmidt VH, Zhang R, Cao W, Luo H. J. Appl. Phys. 2004; 96:549.
51. Zhang SJ, Lebrun L, Randall CA, Shrout TR. Phys. Stat. Sol. (a). 2005; 202:151.
52. Yamada T. J. Appl. Phys. 1972; 43:328.
53. Damjanovic D. Phys. Rev. B. 1997; 55:R649.
54. Li F, Zhang SJ, Lin DB, Luo J, Zhuo X, Wei XY, Shrout TR. J. Appl. Phys. 2011:109. in press.

55. Davis M, Damjanovic D, Setter N. Phys. Rev. B. 2006; 73 014115.
56. Li F, Zhang SJ, Xu Z, Wei X, Luo J, Shrout TR. Appl. Phys. Lett. 2010; 96 192903.
57. Paik DS, Park SE, Shrout TR. J. Mater. Sci. 1999; 34:469.
58. Jiang, X.; Rehrig, PW.; Hackenberger, WS.; Shrout, TR. AIP Conf. Proc; 2006. p. 1783
59. Jaffe, B.; Cook, WR.; Jaffe, H. Piezoelectric Ceramics. London and New York: Academic; 1971.
60. Zhang SJ, Li F, Luo J, Xia R, Hackenberger W, Shrout TR. IEEE Trans. Ultrason. Ferro. Freq. Contr. 2011; 58 in press.
61. Zhang SJ, Sherlock NP, Meyer RJ Jr, Shrout TR. Appl. Phys. Lett. 2009; 94 162906.
62. Li, F.; Zhang, S.; Luo, J.; Hackenberger, W.; Shrout, TR. Electromechanical Properties of Tetragonal $\text{Pb}(\text{In}_{1/2}\text{Nb}_{1/2})\text{O}_3\text{-Pb}(\text{Mg}_{1/3}\text{Nb}_{2/3})\text{O}_3\text{-PbTiO}_3$ crystals. US Navy Workshop on Acoustic Transduction Materials and Devices; The Penn State Conference Center; May, 2010; State College, PA.
63. Sherlock NP, Zhang SJ, Luo J, Lee HY, Shrout TR, Meyer RJ Jr. J. Appl. Phys. 2010; 107 074108.
64. Meyer, RJ., Jr; Tremper, TM.; Markley, DC.; Van Tol, D.; Han, P.; Tian, J. Low Profile, Broad-Bandwidth Projector Design Using d_{36} Shear Mode. US Navy Workshop on Acoustic Transduction Materials and Devices; The Penn State Conference Center; May, 2010; State College, PA.

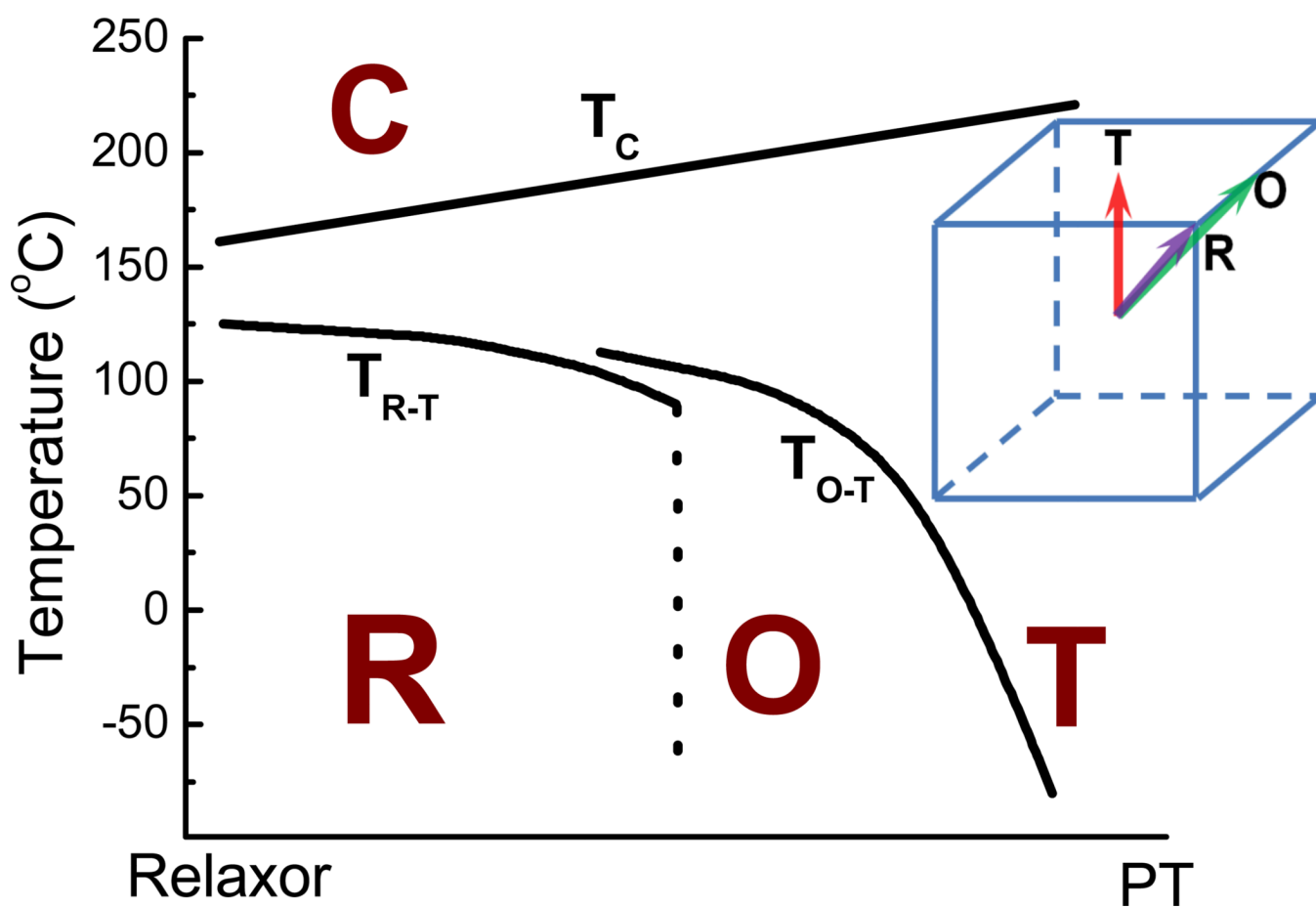


Figure 1. Schematic phase diagram for Relaxor-PT based crystals, where R, O and T represent rhombohedral, orthorhombic/monoclinic (M_C) and tetragonal phase regions, data got from references [33, 54].

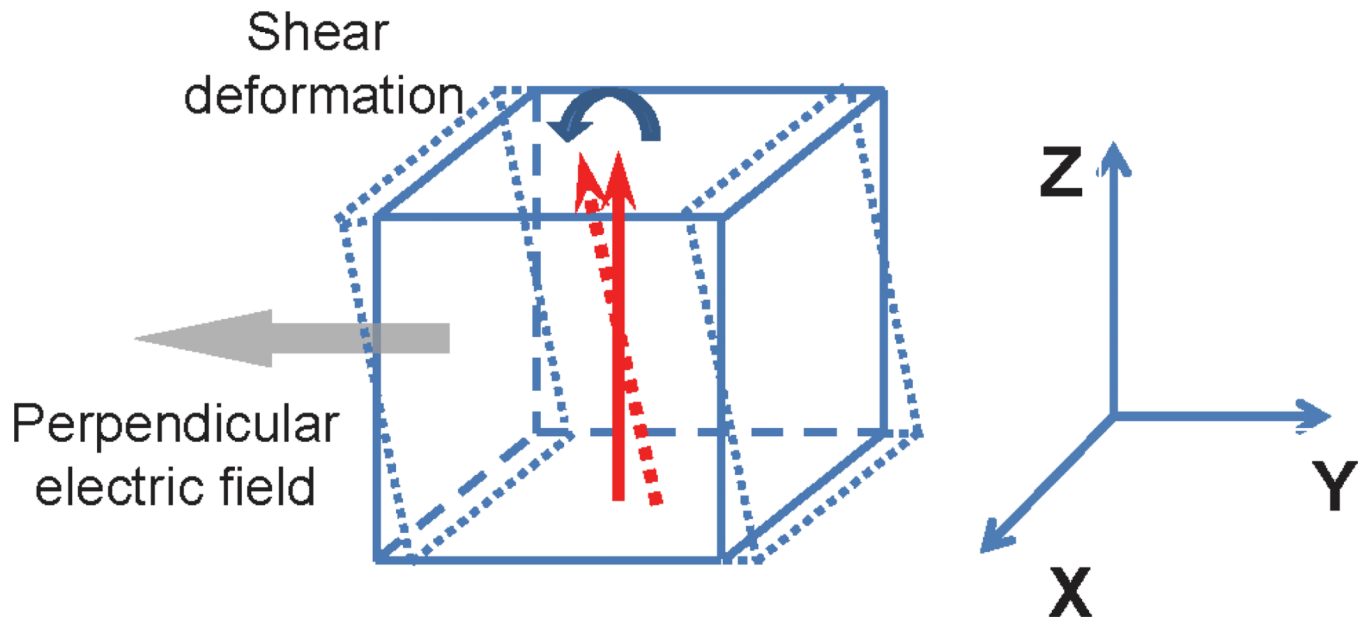


Figure 2. Schematic polarization rotation process and related shear piezoelectric deformation, under perpendicular electric field.

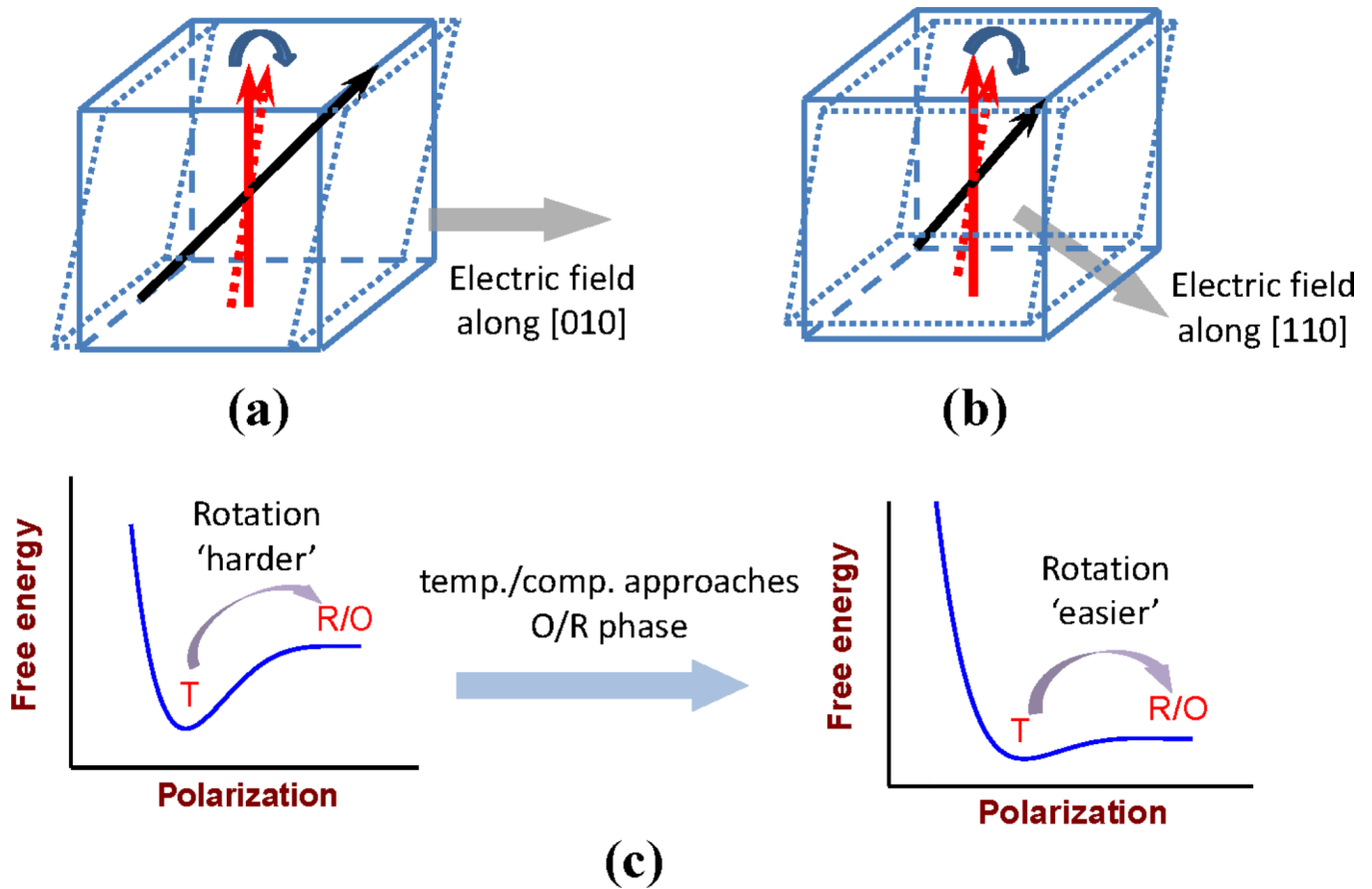


Figure 3.

The shear piezoelectric deformations for tetragonal crystals, corresponding to shear coefficient d_{15} . With applying perpendicular electric field along (a) $[010]_C$ and (b) $[110]_C$, polarization rotates to $[011]_C$ (polar direction of orthorhombic phase) and $[111]_C$ direction (polar direction of rhombohedral phase) respectively. The subscript 'C' represents the crystallographic axes in pseudo-Cubic lattice.

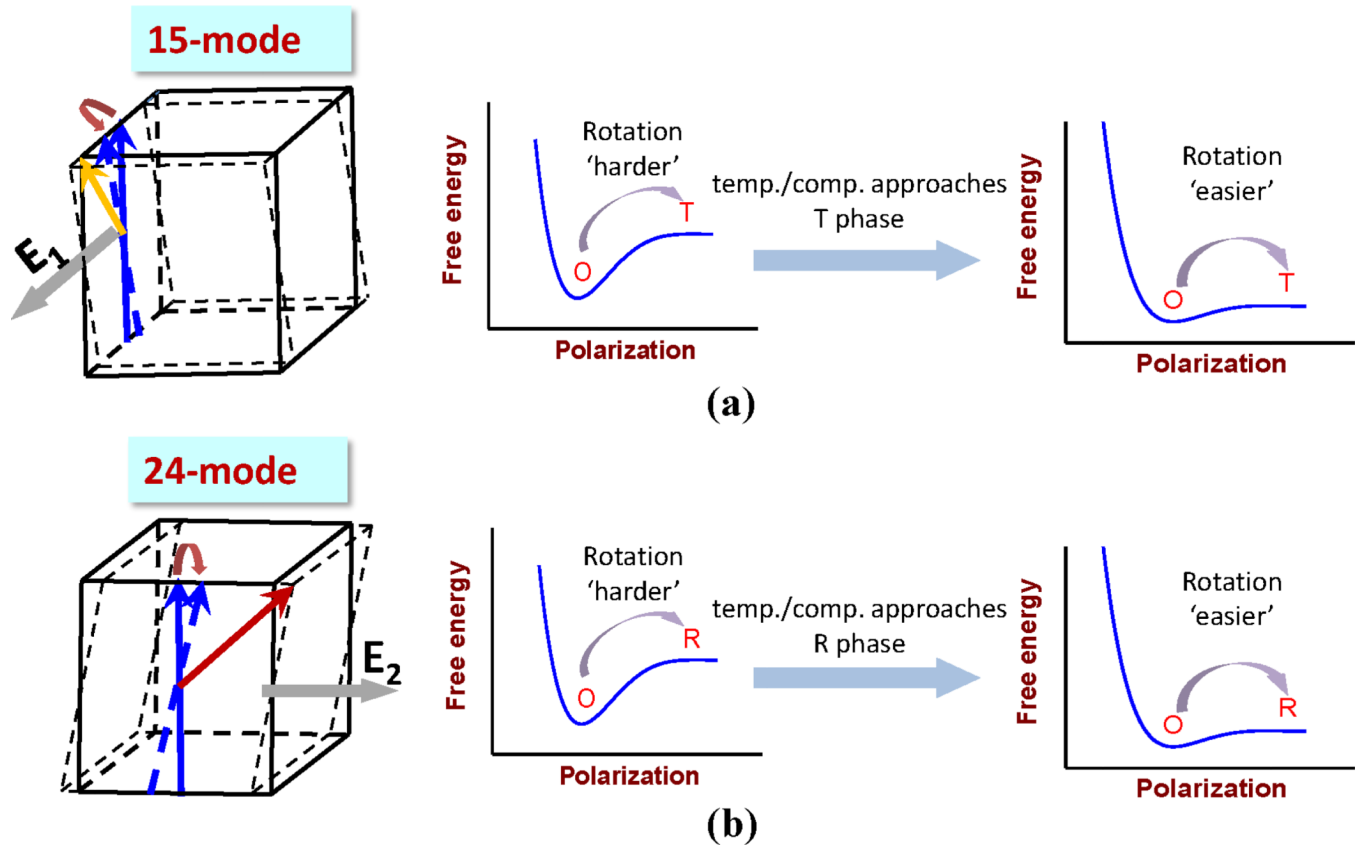


Figure 4. Two independent shear piezoelectric responses (15- and 24-mode) and related polarization rotation path in orthorhombic crystals, where the solid and dotted blue arrows represent the polarization rotation process under perpendicular electric field. The electric field E_1 and E_2 are along $[0\bar{1}1]_C$ and $[100]_C$ directions, respectively. The yellow (a) and brown (b) arrows represent the $[001]_C$ and $[111]_C$ directions, respectively.

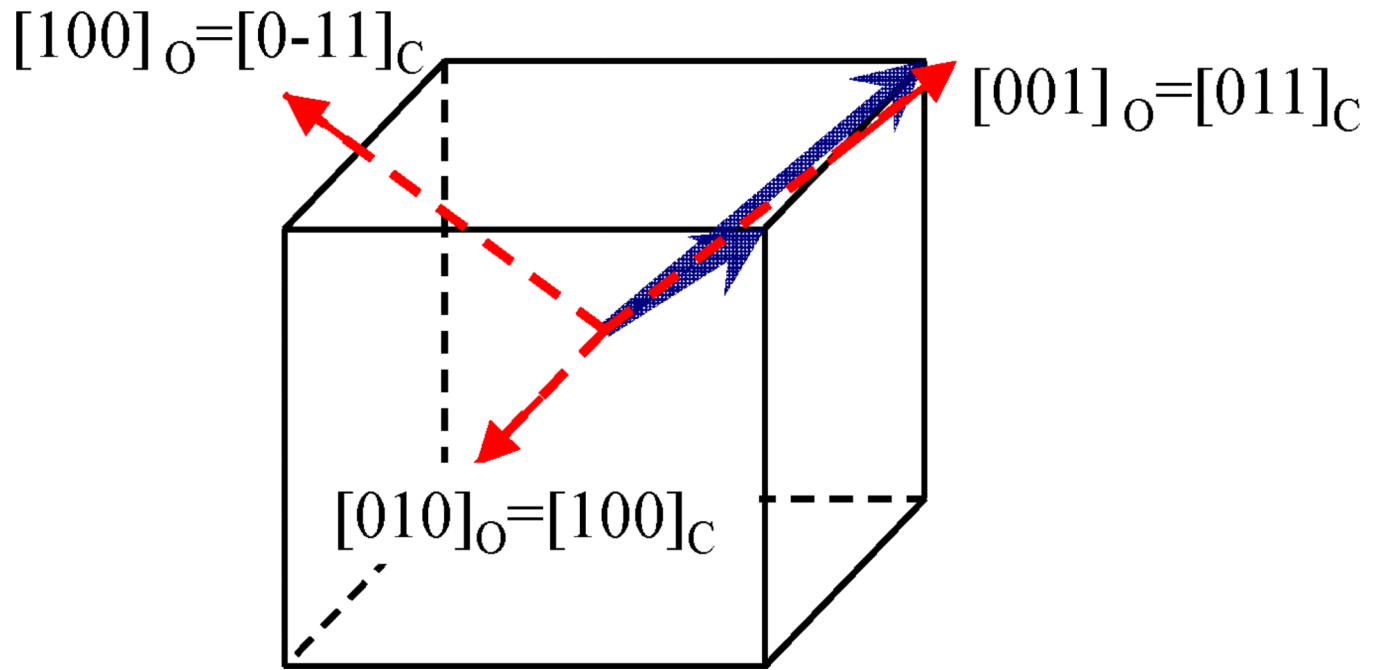


Figure 5. Domain structure of $[011]_C$ poled rhombohedral crystals, where the blue arrows represent the two different rhombohedral domains. The subscript 'O' represents the crystallographic axes in orthorhombic lattice.

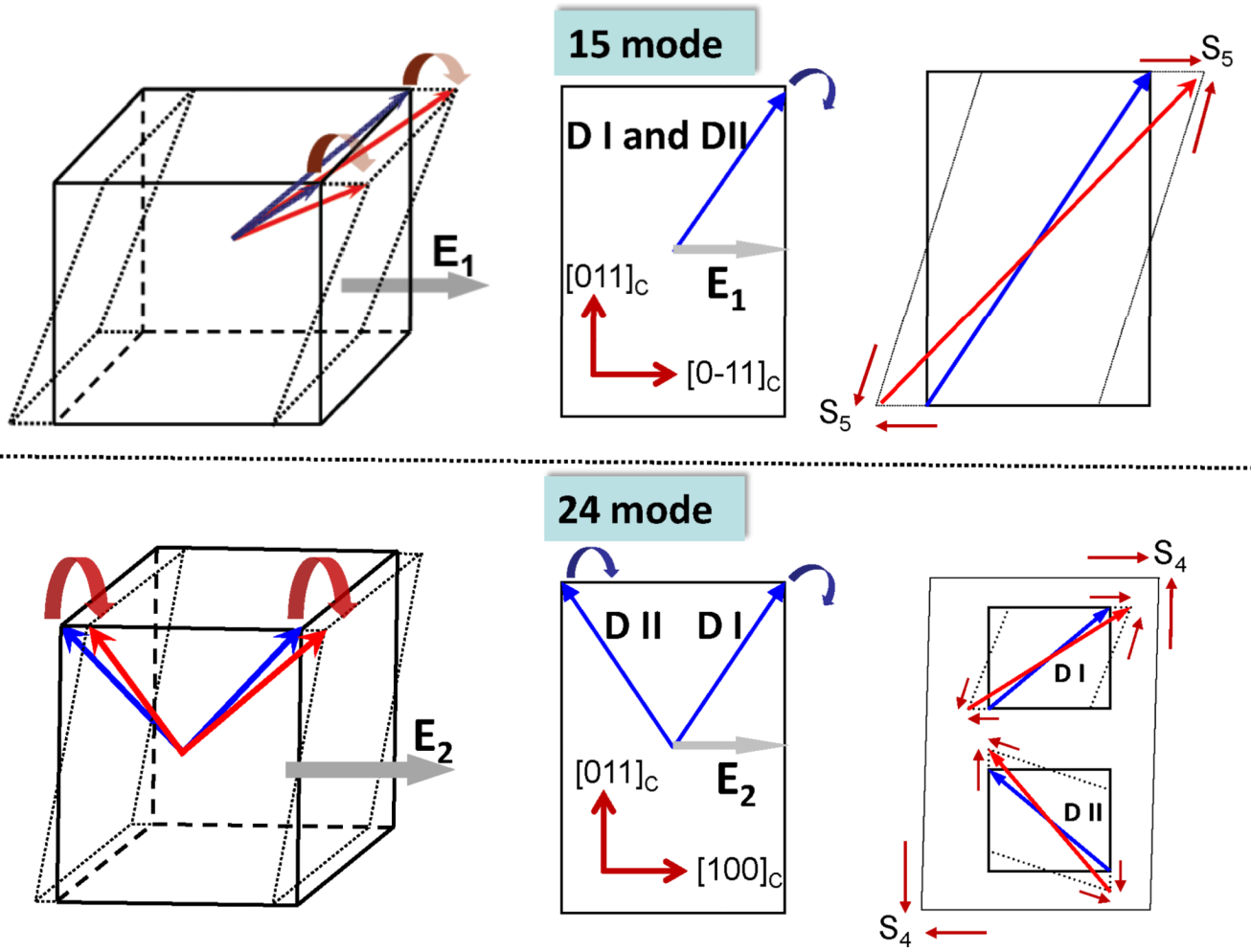


Figure 6. Shear piezoelectric behaviors and related polarization rotation process for $[011]_C$ poled rhombohedral crystals.

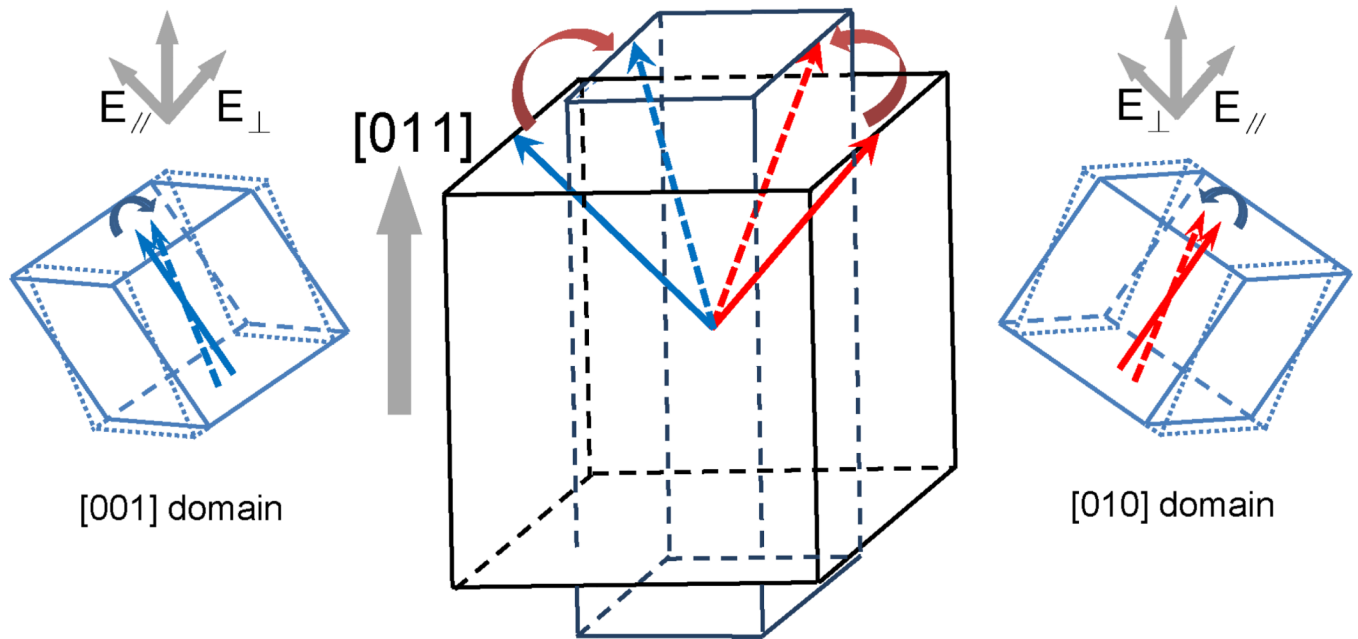


Figure 7. Schematic figure of the piezoelectric deformation in $[011]_C$ poled tetragonal crystals. It can be seen that the shear piezoelectric response of single domain state can contribute to the longitudinal piezoelectric response of domain engineered crystals.

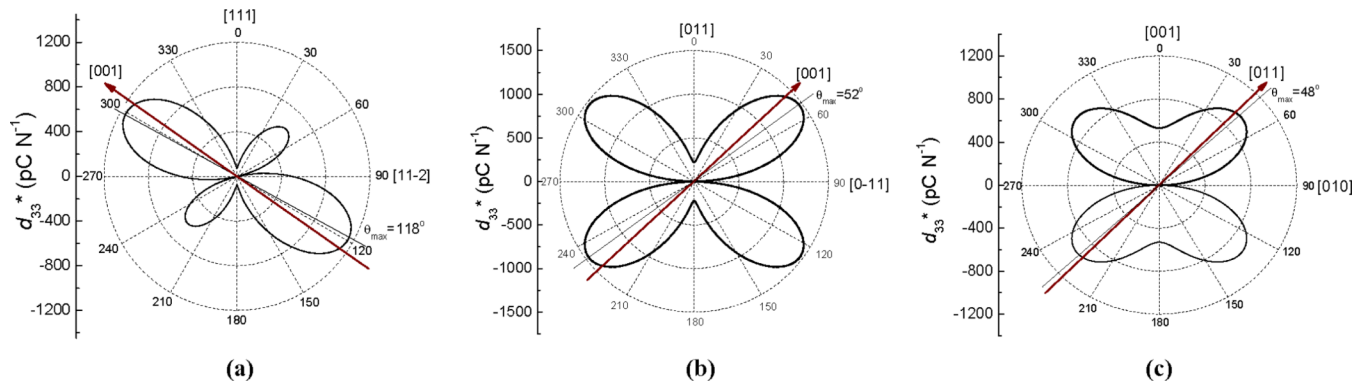


Figure 8.

Orientation dependence of piezoelectric coefficient d_{33}^* for single domain PIN-PMN-PT crystals with (a) rhombohedral, (b) orthorhombic and (c) tetragonal phases, where the input data is from references [49, 47, 33].

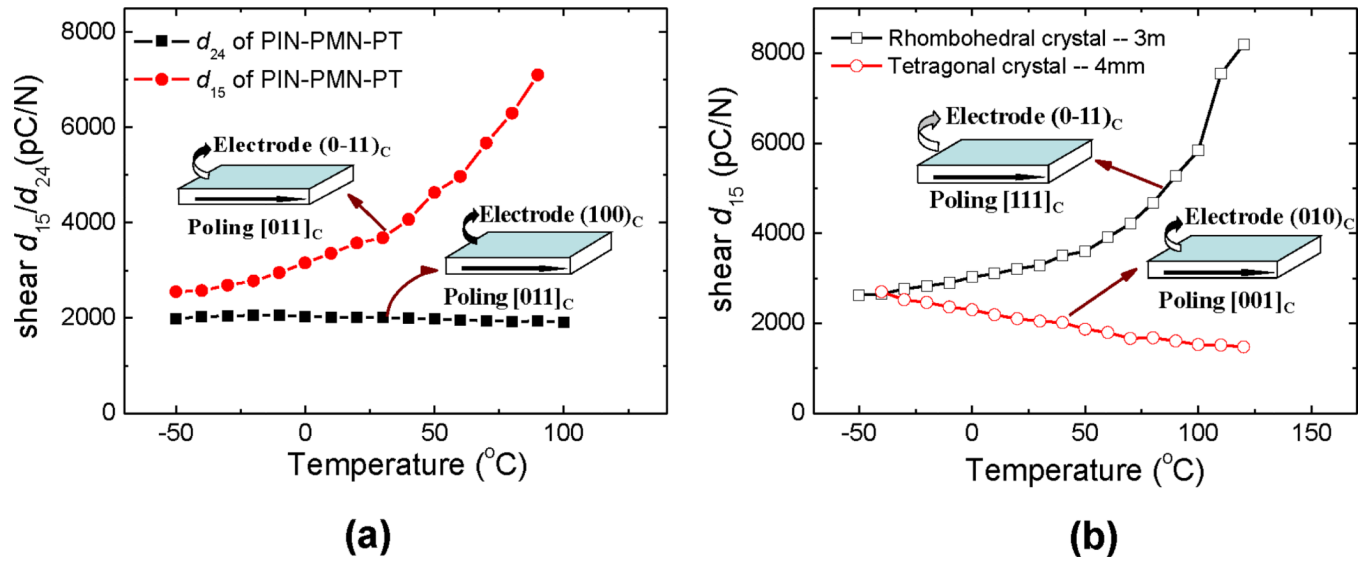


Figure 9. The temperature dependence of shear piezoelectric coefficients for (a) orthorhombic PIN-PMN-PT crystals; (b) rhombohedral and tetragonal PIN-PMN-PT crystals. Reprinted with permission from [40]. Copyright [2010], American Institute of Physics

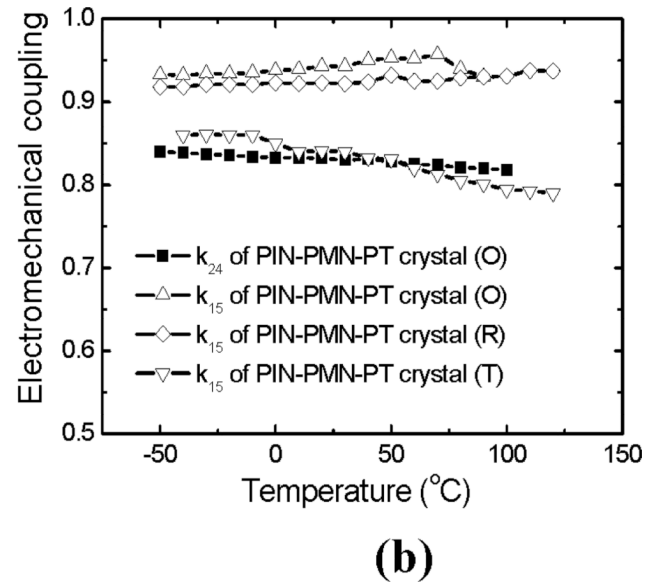
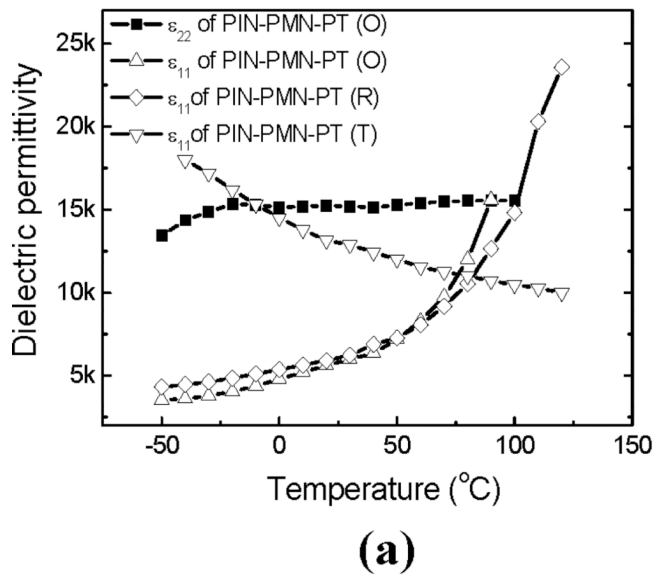


Figure 10. The temperature dependence of (a) transverse dielectric permittivity and (b) shear electromechanical couplings for PIN-PMN-PT crystals.

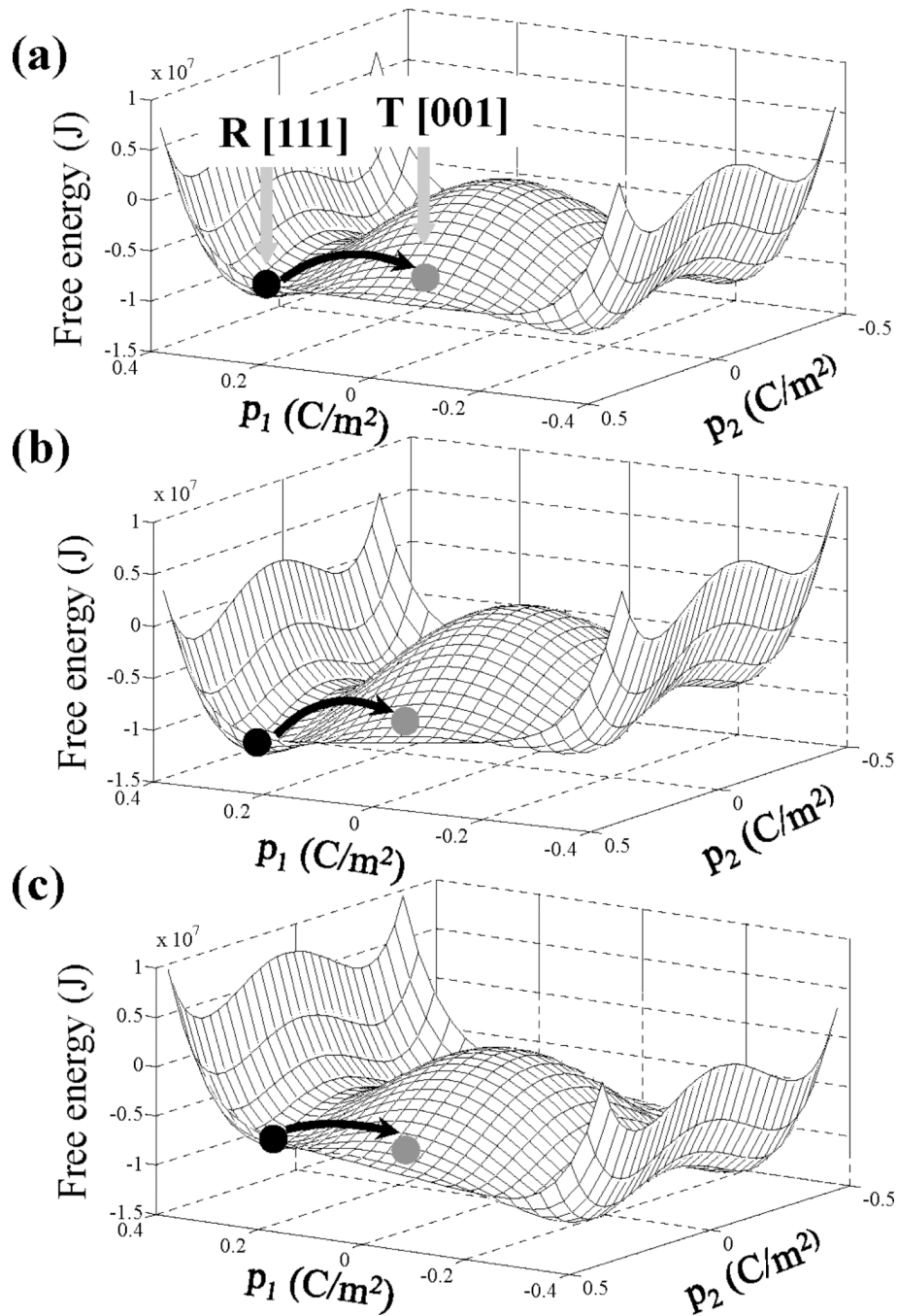


Figure 11.

Gibbs free energy profile for PZT60/40 (Zr/Ti=60/40) at (a) zero bias field, (b) 50kV/cm along [111] direction (parallel electric field), (c) 50kV/cm along [-1-12] direction (perpendicular electric field). At the above conditions, polarization p_x and p_y are equivalent for the free energy of PZT60/40. Thus, the free energies are plotted with respect to polar vectors p_1 and p_2 , where $p_x=p_y=p_1$, $p_z=p_2$. The coefficients in Eq. (1) were obtained from reference [42].

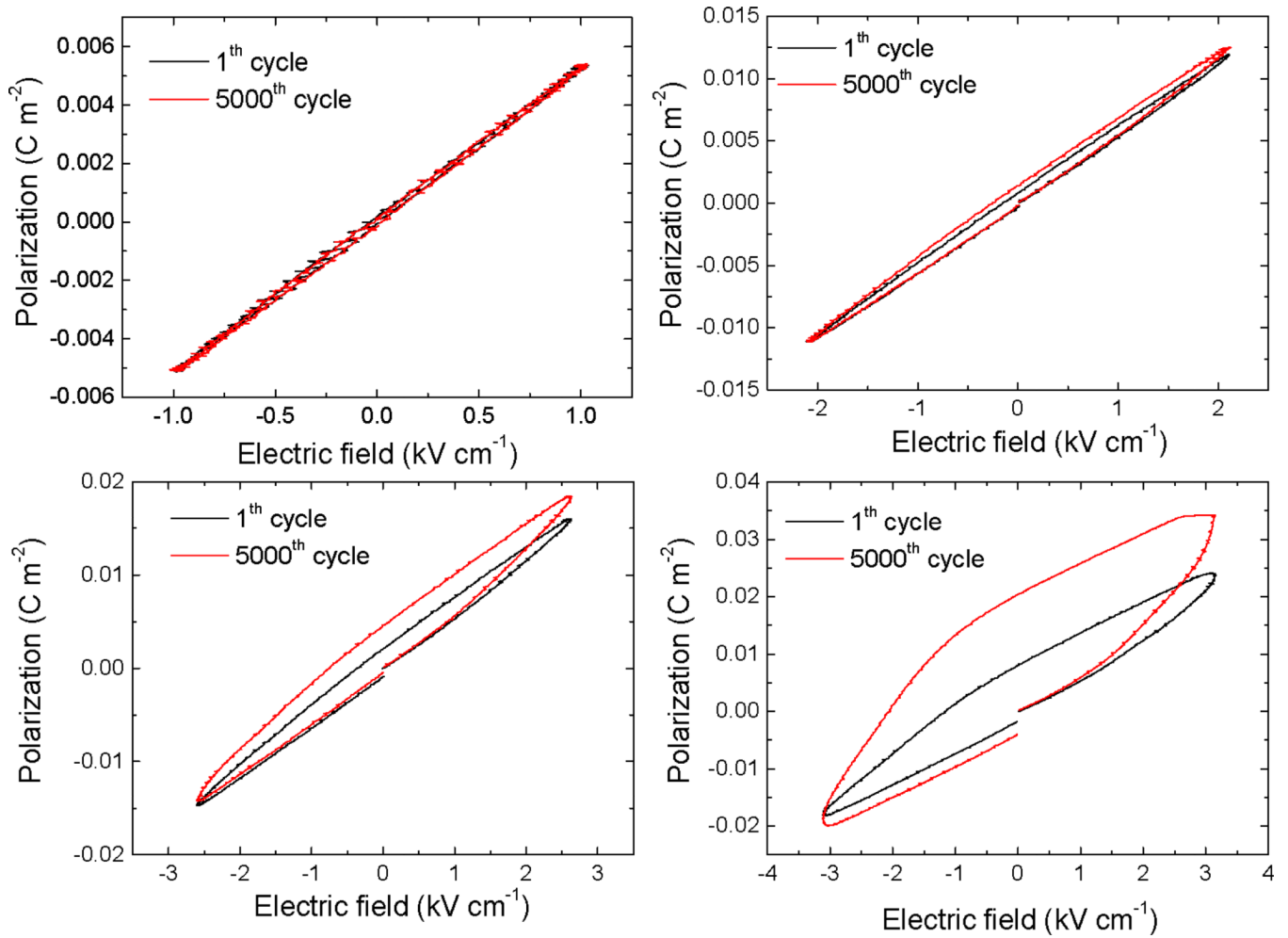


Figure 12.

The polarization vs electric field behaviors for $[111]_{\text{C}}$ poled rhombohedral PIN-PMN-PT crystals under various levels of electric field, where the ac field was applied on the $(-110)_{\text{C}}$ faces.

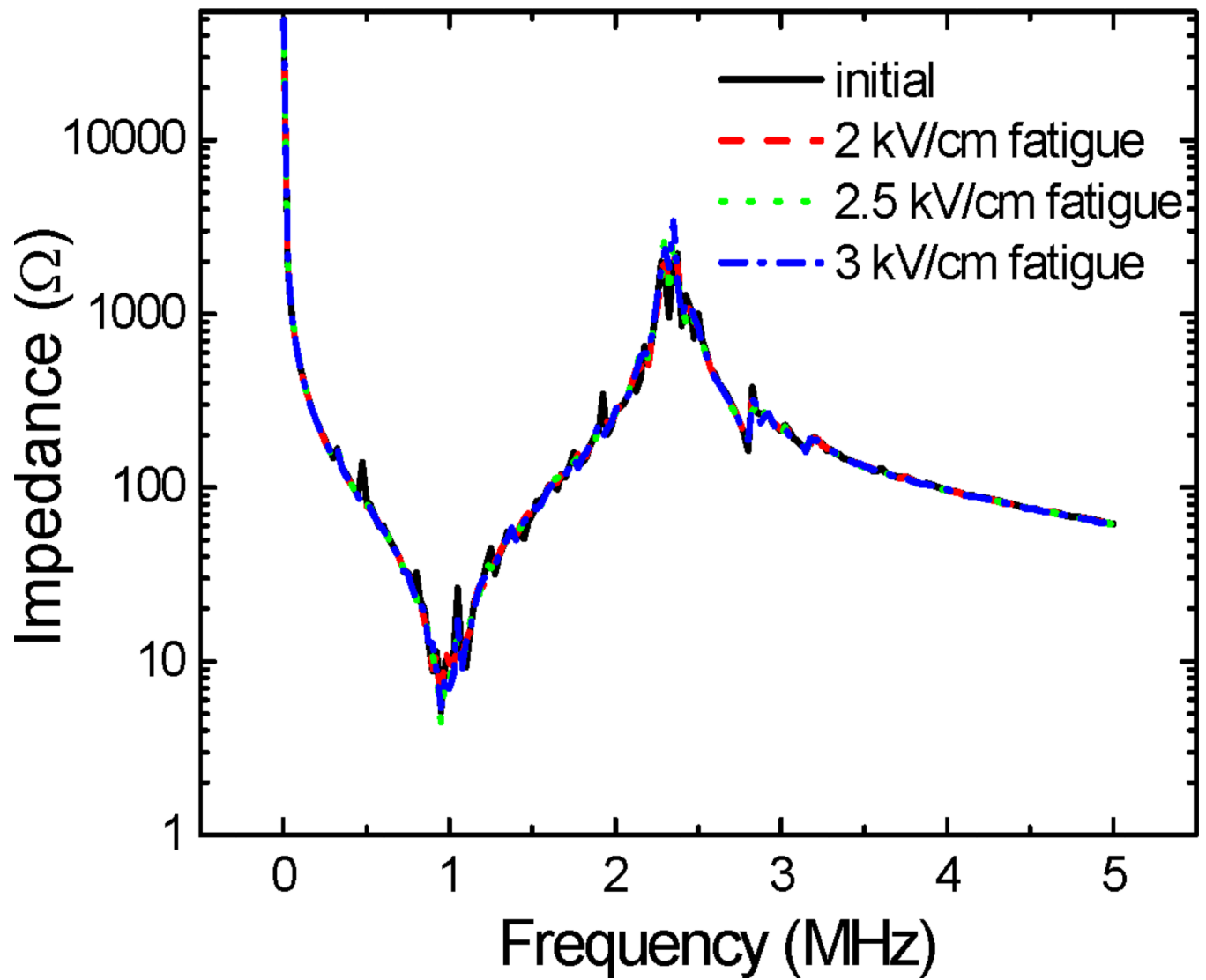


Figure 13. The impedance spectrum of PIN-PMN-PT crystals with shear vibration mode, where the impedance spectrums were measured after 5000th cycling at various levels of ac field.

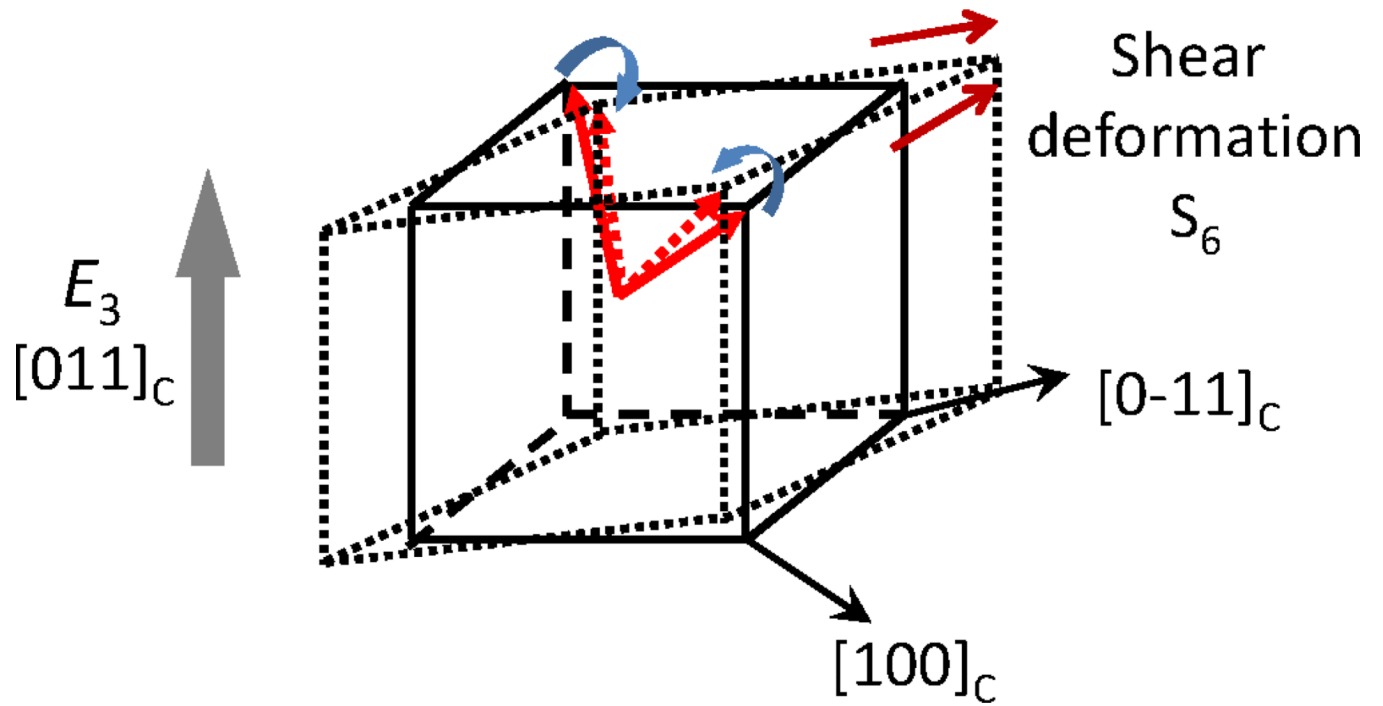


Figure 14. Schematic polarization rotation process and related shear piezoelectric deformation for 36-mode, where the red arrows represent the spontaneous polar vector $[-111]$ and $[111]$ of rhombohedral crystals.

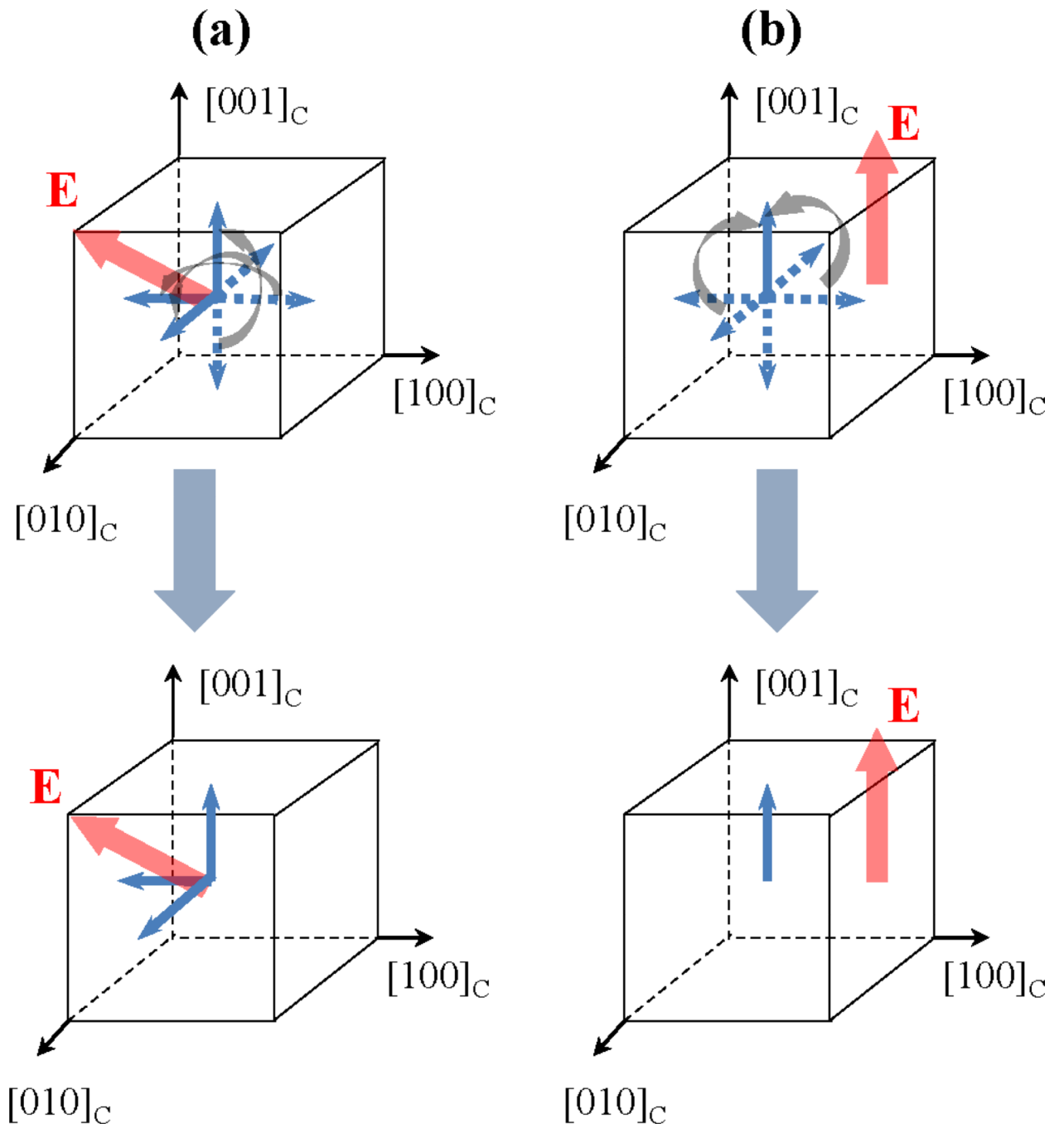


Figure 15. Domain evolution of tetragonal crystals by poling along (a) [111] direction (b) [001] direction.

Table 1

Electromechanical shear properties for PIN-PMN-PT crystals with rhombohedral, orthorhombic, and tetragonal phases.

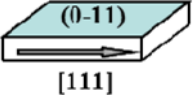
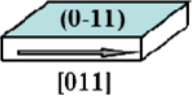
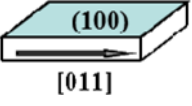
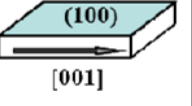
Phase	Rhombohedral	Orthorhombic		Tetragonal
 Poling  Electrode				
Domain Configuration	1R	1O	1O	1T
Symmetry	3m	mm2	mm2	4mm
Properties	$d_{15} > 3000 \text{ pC N}^{-1}$ $k_{15} > 90\%$ $\epsilon_{11} > 6000$ $s_{55}^D \sim 27 \text{ pm}^2 \text{ N}^{-1}$	$d_{15} > 3000 \text{ pC N}^{-1}$ $k_{15} > 90\%$ $\epsilon_{11} > 6000$ $s_{55}^D \sim 26 \text{ pm}^2 \text{ N}^{-1}$	$d_{24} \sim 2000 \text{ pC N}^{-1}$ $k_{24} > 85\%$ $\epsilon_{22} > 15000$ $s_{55}^D \sim 15 \text{ pm}^2 \text{ N}^{-1}$	$d_{15} \sim 2000 \text{ pC N}^{-1}$ $k_{15} \sim 80\%$ $\epsilon_{11} > 12000$ $s_{55}^D \sim 15 \text{ pm}^2 \text{ N}^{-1}$

Table 2

Piezoelectric and dielectric anisotropies of relaxor-PT based crystals with various phases.

Relaxor-PT crystals	Data for single domain state						Engineered domain configuration
	ϵ_{33}/ϵ_0	ϵ_{11}/ϵ_0	$\epsilon_{11}/\epsilon_{33}$	d_{33} [pC N ⁻¹]	d_{15} [pC N ⁻¹]	d_{15}/d_{33}	
PIMNT(T) ^a	1090	15000	14	530	2350	4	84% 75% along [011]
PIMNT(O) ^b	900	5400	6	340	3800	11	82% 93% along [001]
PIMNT(R) ^c	700	6300	9	74	2190	30	36% 89% along [001]
PMN-0.42PT(T) ^d	660	8600	13	260	1300	5	78% 72% along [011]
PMN-0.33PT(R) ^e	640	3900	6	190	4100	21	69% 94% along [001]
PZNT-0.12PT(T) ^f	870	12000 ^g	14	560	1450 ^g	2.5	87% 62% along [011]
PZNT-0.08PT(R) ^g	1000	16000	16	90 ^g	5000	55	39% 94% along [001]

^a reference [33] and [48];

^b reference [47];

^c reference [49];

^d reference [50];

^e reference [39];

^f reference [51];

^g reference [1] and [37]

Table 3

Ac field stability and related properties for PIN-PMN-PT crystals. After reference [60].

^a : poling direction ^b : electrode surface	Domain configuration	material	E_C [kV cm ⁻¹]	E_{mit} [kV cm ⁻¹]	ϵ	s^D [pm ² N ⁻¹]	d_{15} [pC N ⁻¹]	k_{15}	N_r [Hz m]	Ac field stability [kV cm ⁻¹]	Q
[111] ^a /(1-10) ^b	1R	Pure PIN	4.5	0	6000	27	3500	0.93	470	2	30
		Mn-PIN	6.2	1.0	8000	26	4100	0.94	410	4	32
[011] ^a /(0-11) ^b	1O	Pure PIN	5.5	0	5600	27	3400	0.95	380	2	20
		Mn-PIN	8.9	0.6	5800	27	3500	0.95	360	5	25
[001] ^a /(100) ^b	1T	Pure PIN	11.0	0	15000	14	2200	0.85	850	4	20
		Mn-PIN	11.5	1.5	8000	14	1200	0.77	950	6	33